Ultrastructural Characterization of Stem Cell-Derived Replacement Vestibular Hair Cells Within Ototoxin-Damaged Rat Utricle Explants

MIMMI WERNER [ID],[1*] THOMAS R. VAN DE WATER [ID],[2]
HANS STENLUND,[3] AND DIANA BERGGREN[1]
[1]Department of Clinical Sciences, Otolaryngology, University of Umeå, Umeå, Sweden
[2]Cochlear Implant Research Program, Department of Otolaryngology, University of Miami
Ear Institute, University of Miami Miller School of Medicine, Miami, Florida
[3]Department of Epidemiology and Global Health, University of Umeå, Umeå, Sweden

ABSTRACT

The auditory apparatus of the inner ear does not show turnover of sensory hair cells (HCs) in adult mammals; in contrast, there are many observations supporting low-level turnover of vestibular HCs within the balance organs of mammalian inner ears. This low-level renewal of vestibular HCs exists during normal conditions and it is further enhanced after trauma-induced loss of these HCs. The main process for renewal of HCs within mammalian vestibular epithelia is a conversion/transdifferentiation of existing supporting cells (SCs) into replacement HCs.In earlier studies using long-term organ cultures of postnatal rat macula utriculi, HC loss induced by gentamicin resulted in an initial substantial decline in HC density followed by a significant increase in the proportion of HCs to SCs indicating the production of replacement HCs. In the present study, using the same model of ototoxic damage to study renewal of vestibular HCs, we focus on the ultrastructural characteristics of SCs undergoing transdifferentiation into new HCs. Our objective was to search for morphological signs of SC plasticity during this process. In the utricular epithelia, we observed immature HCs, which appear to be SCs transdifferentiating into HCs. These bridge SCs have unique morphological features characterized by formation of foot processes, basal accumulation of mitochondria, and an increased amount of connections with nearby SCs. No gap junctions were observed on these transitional cells. The tight junction seals were morphologically intact in both control and gentamicin-exposed explants. Anat Rec, 303:506–515, 2020. © 2019 The Authors. *The Anatomical Record* published by Wiley Periodicals, Inc. on behalf of American Association of Anatomists.

The inner ear sensory epithelium for hearing (cochlea) and balance (vestibule) receptors consists of specialized mechanosensory receptor cells, i.e., hair cells (HCs), and their nonsensory surrounding support cells (SCs). HCs in the vestibular receptors contribute to our sense of balance by registering changes in head position. Loud sounds, aging, infections, and drugs such as cytostatic and aminoglycoside antibiotics can damage and even initiate the death of inner ear HCs. HCs are highly differentiated sensory cells that have lost their ability to proliferate and damage to these sensory cells will therefore lead to impaired hearing and balance. In mammalian vestibular epithelia, but not in the cochlear epithelium, a limited spontaneous renewal of HCs can be induced by a trauma causing HC-loss such as aminoglycoside exposure (Forge et al., 1993; Tanyeri et al., 1995; Forge et al., 1998; Berggren et al., 2003; Werner et al., 2015). The process contributing to the renewal of mammalian vestibular HCs after aminoglycoside exposure has been described as a direct transdifferentiation of SCs into HCs (Kawamoto et al., 2009; Lin et al., 2011; Burns and Stone, 2017). Furthermore, there is limited spontaneous proliferation among the SCs after aminoglycoside-induced trauma to the vestibular epithelia *in vitro* but there is no evidence that this mechanism gives rise to new HCs (Berggren et al., 2003; Kawamoto et al., 2009).

Recent studies have shown that there is a subgroup of SCs, i.e., those expressing the Wnt target gene Lgr5, that have the ability to act as HC progenitors after a loss of HCs (Bramhall et al., 2014; Cox et al., 2014; Lin et al., 2015). During the process of direct transdifferentiation of an SC into an HC, the SC appears to undergo a sequential series of changes in its phenotypic features. Morphologically, this process of direct transdifferentiation has been observed to occur gradually *in vitro* and cells that show both SC and HC characteristics have been identified (Li and Forge, 1997; Werner et al., 2015).

In the vestibular epithelium of macula utriculi, the HCs do not contact the basal membrane and are isolated from one another by interspaced SC projections. The basal part of the SCs contact the basal membrane and their cell bodies span through the entire epithelium. The nuclei of the SCs are lined up close to the basal membrane, whereas the HC nuclei are located in a more apical position (Fig. 1). The SC area has been described as a syncytium (Kawamoto et al., 2009) and the SCs appear to have a rich and rapid communication network with each other (Jagger et al., 2014). The HCs that are surrounded by the SCs do not seem to participate in the communication network of the SCs. A prerequisite for a rapid communication network is numerous connections between the cells usually by gap junctions (GJs). GJs act as electronic couplers between the SCs allowing ions, electrical currents, and macromolecules to pass through these protein channels, i.e., connexons, from one cell to another. Numerous GJs have been found between SCs below the level of the tight junctions (TJs) in both the auditory and the vestibular parts of the inner ear in

several species of animals (Forge et al., 2003). Forge and colleagues did not find any GJs between HCs and SCs using thin sections studied with transmission electron microscopy (TEM) and in freeze fracture preparations (Forge et al., 2003). These observations raise the question whether the subgroup of SCs that have the ability to act as HC progenitors and transdifferentiate into HCs do participate in the communication network of the other SCs or not. If they do participate and have GJs as the other SCs, all their GJs would have to degenerate during the process of transdifferentiation into HCs. During development, a permanent degeneration of GJs on certain cells occur, since it has been shown for mice that
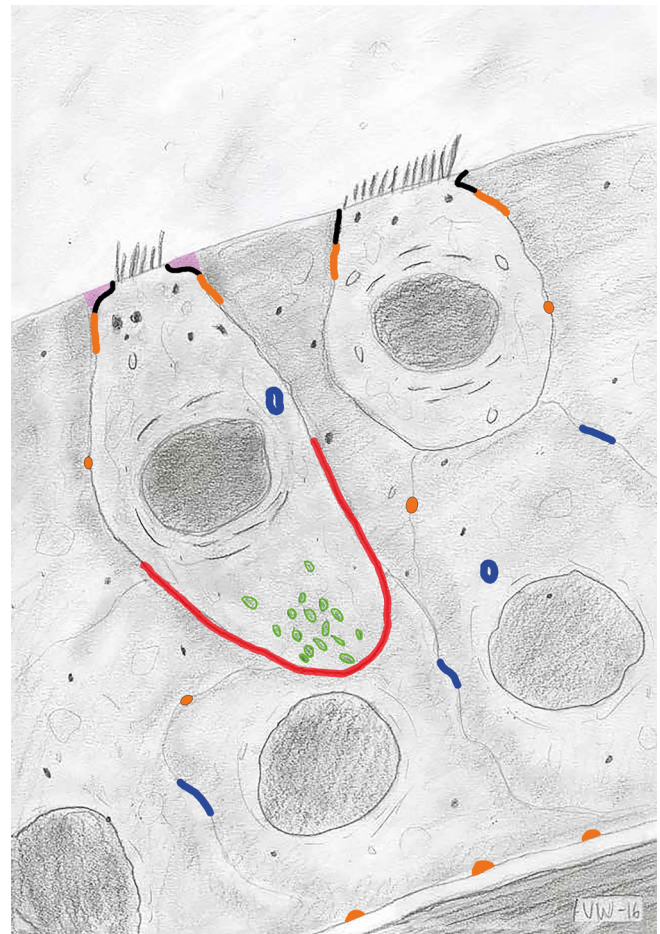
Fig. 1. Schematic figure illustrating our morphological findings in utricular epithelia during direct transdifferentiation. The HC to the right illustrates a normal mature HC. The HC to the left illustrates a cell with characteristics of a former SC transdifferentiating into a HC. Black line apically; TJ, orange line; AJ, orange dot; DS, blue line; GJ, blue circle; intracellular annular junction, purple area; SC extension, red line; outlining basal extension, green circles; assembly of mitochondria basally in foot process.

GJs are present on all cells in the inner ear sensory epithelium until the 15th to 16th gestational day but from the 19th gestational day on GJs could not be found in association with HCs (Bagger-Sjoback and Anniko, 1984).

Except from GJs, three further types of intercellular junctions have been characterized in the vestibular epithelial tissue: TJs, adherent junctions (AJs), and desmosomes (DSs) (Bagger-Sjoback and Anniko, 1984; Forge et al., 2003; Kim et al., 2005). TJs, AJs, and DSs are not known to act as communication sites between cells but rather to have closing functions, maintaining integrity at the luminal surface and the adhesion between cells intact. TJs line the entire luminal surface of vestibular sensory epithelia and act as a diffusion barrier. AJs, located beneath the TJs, have adhesion functions and there are actin filaments associated with AJs that are important in initiating contraction of the apical surface of the cell. DSs are dispersed spot-like buttons of adhesion located beneath the AJs. For an ordinary SC, spanning from the basal membrane to the luminal surface, the process of transdifferentiation into an HC would include disruption of the adhesion to the basal membrane and to the basal area of neighboring SCs.

The aim of this study is to systematically investigate ultrastructural characteristics of cells in the process of transdifferentiation from SCs into HCs in cultures of postnatal rat utricular epithelia following ototoxin-damage induced HC-renewal, and to evaluate the presence of intercellular junctions during this process of transdifferentiation.

METHODS

Animals

Litters of 4-day-old (P4) Wistar rat pups with a nursing mother were obtained from Charles River Laboratories. The P4 rats stayed with their mothers until shortly before they were euthanized by rapid cervical dislocation and used for preparations of organotypic cultures of dissected utricles. The care and use of animals was approved by the Regional Care and Use Committee of the University of Umeå (A 49-08) and conformed to NIH guidelines for the care and use of laboratory animals.

Organ Culture

The heads of the P4 rats were sprayed with 70% ethanol. The temporal bones were removed and the capsule covering the vestibule was opened. Utricular maculae were excised as a unit and their otoconial membranes were gently removed. The explanted utricles were composed of the complete macular epithelium with retention of a minimal amount of subepithelial mesenchyme tissue. The dissection was performed in Dulbecco's phosphate-buffered saline supplemented with glucose (6 g/L) maintained at room temperature. The explants were placed with their epithelial surfaces uppermost on perforated insert membranes (Transwell Clear membranes with pore size 0.4 µm; Costar, Cambridge, MA). The inserts were placed in 6-well-plates containing Dulbecco's Modified Eagles Medium supplemented with glucose to a final concentration of 6 g/L, 10% fetal bovine serum, N-1 supplement (Sigma) was added at 100 µL to 10 mL of medium, and penicillin (100 U/ml). By reducing the depth of the nutrient medium above the insert membrane, the explants became flattened and anchored to the culture insert membrane. The explants were incubated at 37°C in a humidified 5% carbon dioxide atmosphere and the medium was renewed on every second day.

Culture Paradigms

The day of explantation was denoted as day zero in vitro (0 DIV). Explants were cultured for up to 28 DIV. During the initial 48 hr of incubation, all explants were cultured in medium without gentamicin to allow the explants to adhere to the insert membrane and to allow for recovery from any damage incurred during the surgical excision and transfer to organotypic culture. On the second day in vitro (2 DIV), the explanted utricular maculae were divided into two groups, a control group (Group C) and a gentamicin-exposed group (Group G), and were cultured for up to 28 DIV. Group C, explants were cultured in nutrient medium without any drugs added throughout the experiment. Group G macular explants were exposed to 1 mM gentamicin (Sigma, G-3632) for 48 hr (i.e., during in vitro days 2 and 3), and then the gentamicin was washed out and these G explants were allowed to recover. Eighteen utricular explants, eight from Group C, and ten from Group G were used for morphological observations with the aid of TEM (Table 1). Some of the TEM grids were obtained from reembedded plastic light microscopic (LM) sections.

Tissue Processing

While still attached to the insert membrane, the explants were fixed with 2.5% glutaraldehyde in 0.1 M sodium cacodylate buffer, and postfixed with 1% osmium tetroxide followed by 1% uranyl acetate. Thereafter, samples on cutout pieces of the culture insert membrane were placed in 70% ethanol and dehydrated in series of graded ethanol followed by propylene, and finally a solution of propylene and Poly/Bed (50:50). The maculae, still attached to a piece of the membrane, were then embedded in Poly/Bed (Polysciences Inc., Warrington, PA).

Preparation of Sections for Transmission Electron Microscopy

One-micrometer plastic LM sections (chosen for TEM analysis) were photodocumented and then reembedded for TEM by using the method of King and coworkers (King et al., 1982). In brief, the sections were placed in xylene for 24 hr and then rinsed in 100% ethanol. They were then placed in acetone for 1 hr. Beem capsules filled with unpolymerized Poly/Bed were inverted over the sections and polymerized at 60°C. Ultrathin (600 Å) sections were made from the reembedded preparations and from maculae prepared directly for TEM. Sections were mounted

TABLE 1. Distribution of analyzed utricles and HCs

DIV	HCs from Group C	Utricles from Group C	HCs from Group G	Utricles from Group G
2	6	2		
5			8	2
7	7	2	3	1
11			9	2
14	6	1	5	1
17			4	1
21	9	2	12	2
28	1	1	12	1

on formvar-coated grids, stained with uranyl acetate and lead citrate to enhance contrast, and viewed with a JEOL 1230 TEM equipped with the digital micrograph software.

Collection of Material

Sampling for direct sectioning for TEM was made from two utricles at each time point after 2, 5, 7,14, 21, and 28 DIV in Group C and after 5, 7, 11, 14, 17, 21, and 28 DIV in Group G. Sampling for reembedded TEM sections was made from LM sections with a good technical quality from two utricles at the same time points as for the direct sectioning. TEM images from two of the reembedded preparations have been used in an earlier study, but for the purpose of the present study, the grids were reexamined and new photos are taken. In Group C, 15 out of 29 HCs were from reembedded preparation, and in Group G, the corresponding number was 11 out of 53.

Analysis of HC Characteristics and Cell Junctions

All sampled material was analyzed. Each mature and immature HC with visible nucleus and cell membrane that could be followed from the luminal surface and all the way around the cell were systematically evaluated. Routine photomicrography was performed as follows: a full-frame survey with single-portrayals of each chosen HC from the luminal surface to the bottom part was taken. These overview photos were taken from a total of 82 HCs, 29 HCs from eight utricles in Group C, and 53 HCs from 10 utricles in Group G at various time points *in vitro* (see Table 1). The overview TEM images of the 82 individual HCs were blinded, according to time point *in vitro* and for their Groups C and G identity and were analyzed by two of the authors (MW, DB) separately. The agreement between the two assessors in the blinded characterization of HCs was good (Kappa: foot process = 0.89; apical extensions = 0.74; basal accumulation of mitochondria = 0.84; intra class correlation for the number of SC connections = 0.72). In cases where the individual assessment was not consistent regarding an observation, this was discussed until consensus was reached, before the code for the entire material was revealed.

A systematic morphologic evaluation of each individual HC-image was done regarding TJs of the HC, foot process of the HC, lateral extension(s) of the HC, apical SC extensions covering the HC, accumulation of mitochondria basally in the HC, and number of SCs connecting with the HC (Table 2). To score these characteristics of the HCs, the following classification criteria were used:

Tight junction (TJ): *Abnormal*—a disruption of the TJ with identified intercellular space between the cell membranes. *Normal*—no visible disruption of the TJ.

Foot process: *No foot process*—the HC has a symmetrical ending basally. *Remnant foot process*—the HC has an asymmetrical shape ending basally. *Foot process*—the HC has a cytoplasmic extension in the basal direction at the level below the nuclei.

Lateral extensions: *No lateral extension*—the HC has a symmetrical lateral contour. *Lateral extension*—the HC has a cytoplasmic extension in the lateral direction at the level below the nuclei.

Apical SC extensions covering the HC: *No apical SC extensions covering the HC*—the apical surface of the HC has full contact with the lumen of the epithelia. *Remnant*

TABLE 2. Results from scoring of 29 HCs in Group C and 53 HCs in Group G

DIV	2	5	7		11	14		17		21		28	
Group	C	G	C	G	G	C	G	C	G	C	G	C	G
Assymetrical basal	0/6	2/8 (25%)	0/7	2/3 (67%)	3/9 (33%)	0/6	0/5	0/9	2/4 (50%)	0/9	6/12 (50%)	0/1	7/12 (58%)
Foot process	0/6	0/8	0/7	0/3	0/9	0/6	0/5	0/9	0/4	0/9	1/12 (8.3%)	0/1	2/12 (17%)
Partly covered apically	0/6	3/8 (38%)	0/7	0/3	1/9 (11%)	1/6 (17%)	1/5 (20%)	0/9	1/4 (25%)	0/9	1/12 (8.3%)	0/1	2/12 (17%)
Totally covered apically	0/6	0/8	1/7 (14%)	2/3 (67%)	3/9 (33%)	1/6 (17%)	0/5	0/9	0/4	0/9	4/12 (33%)	0/1	0/12
Basal accumulation of mitochondria	0/6	3/8 (38%)	0/7	3/3 (100%)	7/9 (78%)	1/6 (17%)	1/5 (20%)	0/9	1/4 (25%)	0/9	5/12 (42%)	0/1	9/12 (75%)
More than five connections with SCs	0/6	4/8 (50%)	0/7	1/3 (33%)	3/9 (33%)	1/6 (17%)	0/5	0/9	1/4 (25%)	0/9	5/12 (42%)	0/1	6/12 (50%)
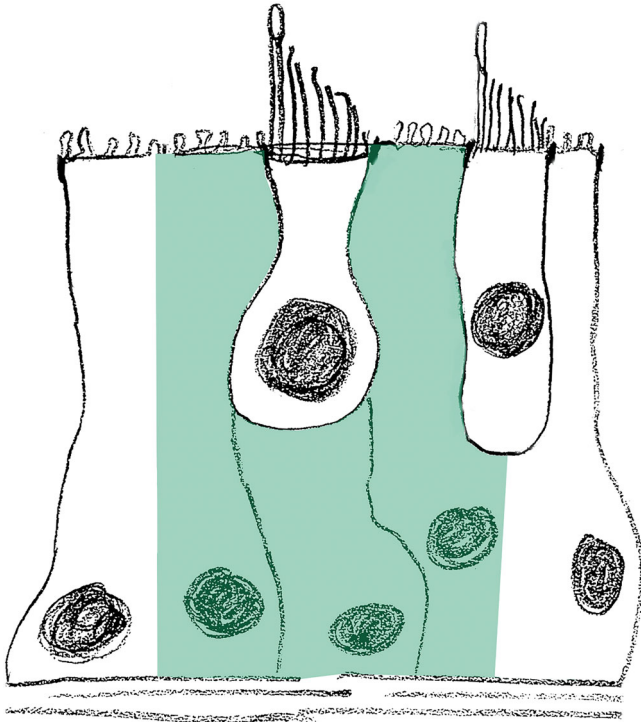
Fig. 2. Schematic illustration of the SC area where screening for intercellular junctions were done.

Fig. 4. TJ between a HC at 17 DIV from Group G and its neighboring SC. The TJ shows a slight abnormal morphology with a distance between the membranes close to the lumen giving it a bubble-like appearance. Asterix marks the area where the TJ seem partly separated.

electron dense area, or a narrowing of the cell membranes of the HC and a neighboring SC, was identified, the area was photodocumented at a magnification of 60,000× to 100,000×.

The SC area was defined by the next SC-SC TJs apically on each side of the chosen HC and lines from those junctions down to the basal membrane (Fig. 2). The SC area around each analyzed HC was searched for cell membranes with a magnification of 20,000×. When an electron dense area, or a narrowing of the cell membranes, was identified, the area was photodocumented at a magnification of 100,000×. The photos at higher magnifications of selected HCs and their adjacent SC area were analyzed, and each identified junction was classified morphologically as either TJ, AJ, DS, or GJ.

apical SC extensions covering the HC—the HC has some contact with the lumen but is partly covered by SC extensions. *Apical SC extensions covering the HC*—the HC has no contact with the lumen and is covered by a layer of SC extensions.

Basal accumulation of mitochondria: *No accumulation of mitochondria basally in the HC. Accumulation of mitochondria basally in the HC.*

Number of SC connections with the HC: *n—number of double-layered cell membranes opposing the double-layered cell membrane of the HC.*

Intercellular junctions in HCs and their SC area were further analyzed by screening in the following manner: The apical side of the HC border to an adjacent SC was photodocumented at higher magnifications, 4,000× to 8,000×. The junctions at each side of the luminary surface of the HC were photodocumented at a magnification of 60,000× to 100,000×. Thereafter, the cell membrane of the HC was observed all around the cell at a magnification of 20,000×. When an

RESULTS

The results from the blinded scoring of HC characteristics from Groups C and G are registered and presented in Table 2 and are illustrated schematically in Fig. 1.

Tight junction (TJ): The TJ seal was classified as morphologically normal apically for all analyzed HCs in Group C and for all analyzed HCs except for one in Group G (see Fig. 3). In Group G, after 17 DIV, one observation was made of a TJ with a slightly abnormal morphology. This HC had a TJ where there was a small distance between the membranes close to the lumen giving it a bubble-like appearance. Above and below this bubble area, the membranes were fused (Fig. 4).

Foot process: None of the 29 HCs analyzed in Group C showed signs of any foot processes. In Group G, 25 out of 53 HCs (47%) had either foot processes or remnants of foot processes, 24 HCs (45%) had no foot process, and in 4 HCs the presence of foot processes could not be assessed (Table 2 and Figs. 5, 6, 7, and 9).

Lateral extensions: No lateral extensions were seen in any of the 29 HCs analyzed in Group C. One HC in Group G after 17 DIV appeared to have a lateral extension toward another HC (Fig. 8).

Apical SC extensions covering the HC: In Group C, 3 out of 29 HCs (10%) had some covering from neighboring SCs apically. In Group G, 18 out of 53 HCs (34%) had some covering from neighboring SCs apically (Table 2 and Figs. 10 and 11). In Group G, there were two HCs where it was not possible to evaluate if they were covered by SCs or not.

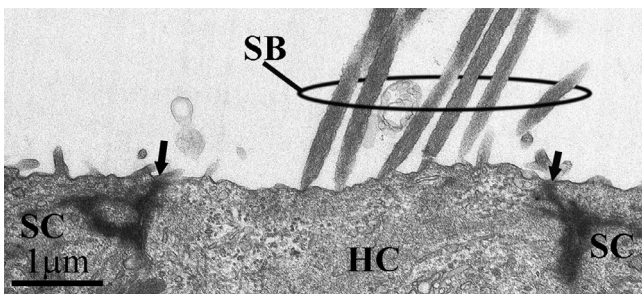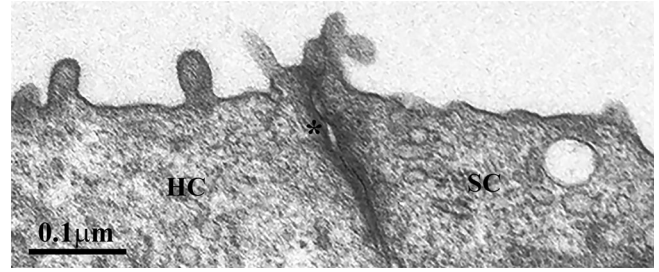**Basal accumulation of mitochondria:** In Group C, 1 out of 29 HCs (3.4%) had a basal accumulation of

Fig. 3. Apical part of a HC at 5 DIV from Group G with morphologically intact TJ seal. Black arrow points at TJ; SB, stereocilia bundle of HC.
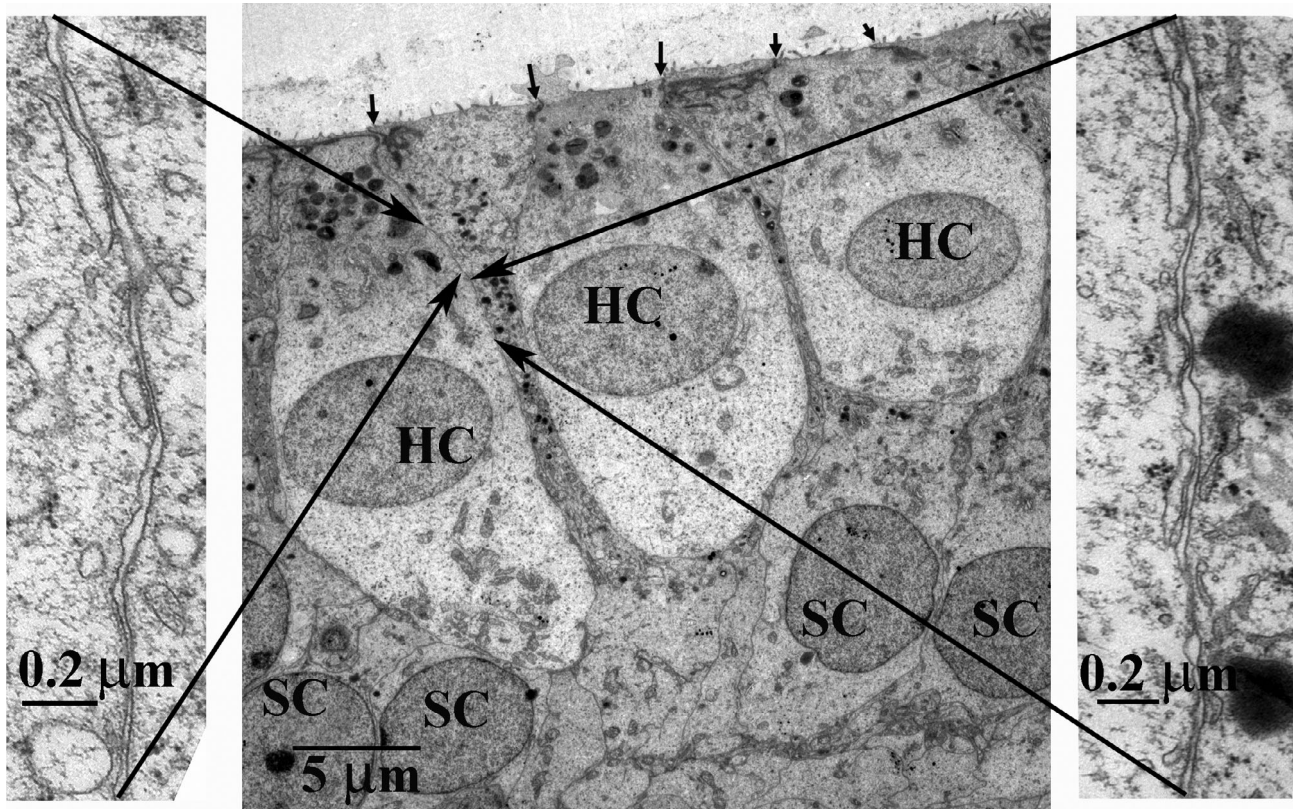
Fig. 5. HCs at 21 DIV from Group G. The HC to the left has a distinct foot-process and basal accumulation of mitochondria. In this cell, there were areas where the distance between the cell membranes occasionally decreased, which were also observed. These tight segments were associated with extra sheets of membrane. Black arrow points at a TJ between a HC and its neighboring SC.

mitochondria. In Group G, 29 out of 53 HCs (55%) had a basal accumulation of mitochondria (Table 2 and Figs. 5–7 and 9).

Number of SC connections with a HC: In Group C, 1 out of 29 HCs (3.4%) had more than five SC connections. In Group G, 20 out of 53 HCs (38%) had more than five SC connections (Table 2 and Figs. 5–7).

In Group C, one or two of the features, foot process, apical SC extensions covering the HC, basal accumulation of mitochondria, or more than five SC connections, were observed in 4 of 30 HCs (13%). In Group G, one to four of these features were observed in 43 of 53 HCs (81%). The simultaneous presence of the three most frequently occurring of these cell characteristics in Group G (foot process, basal accumulation of mitochondria, and more than five SC connections) within the same HC is illustrated in Figure 9.

In Group G, three HCs, one from 21 DIV and two from 28 DIV specimens, had distinct foot processes (Figs. 5–7). All these HCs also showed a basal accumulation of mitochondria. Two of these HCs had foot processes that reached all the way down to the basal membrane and these HCs had 6 and 8–10 SC connections, respectively. The third HC with a well-defined foot process, although it did not reach the basal membrane, had 10–12 SC connections (Fig. 5).

The screening for cell junctions in images of higher magnification of selected HCs and their adjacent SC area resulted in the following observations: TJs, AJs, and DSs were identified between all type of cells, both in Groups C and G, at their luminal borders, and AJs and DSs were also found along the apical lateral sides of SCs and HCs.

The cell membranes of SCs were often hard to follow, since there were many different loops and invaginations, especially in the area beneath the HCs. There were many DSs observed between the SCs and also numerous areas along the SC membranes revealing a GJ-like morphology (Fig. 12). The membranes of the HCs were examined especially for areas with GJ-like morphology but no distinct such areas were found. In Group G specimens, HCs were characterized by the observation that an HC membrane and the membrane of the connecting SC in short segments seemed to fuse in a GJ-like pattern (Fig. 5). The intercellular space between the cell membranes occasionally decreased to 5–15 nm instead of the expected 25–35 nm space. Occasionally, an extra sheet of membrane was observed to be in direct association with these tight segments of the cell membranes (Fig. 5). Vesicles with double membranes possessing the morphological features of GJ plaques were found intracellular in both SCs and HCs in (Fig. 5).

DISCUSSION

Morphologic Characterization of HCs

In this study, we have morphologically identified cells that appear to be in intermediate states during the process of direct transdifferentiation from SCs into HCs. Characteristics for these intermediate cells are basal extensions toward the basal membrane, an assembly of mitochondria close to the cell membrane basally in the cell, and an increased number of SC connections basally.
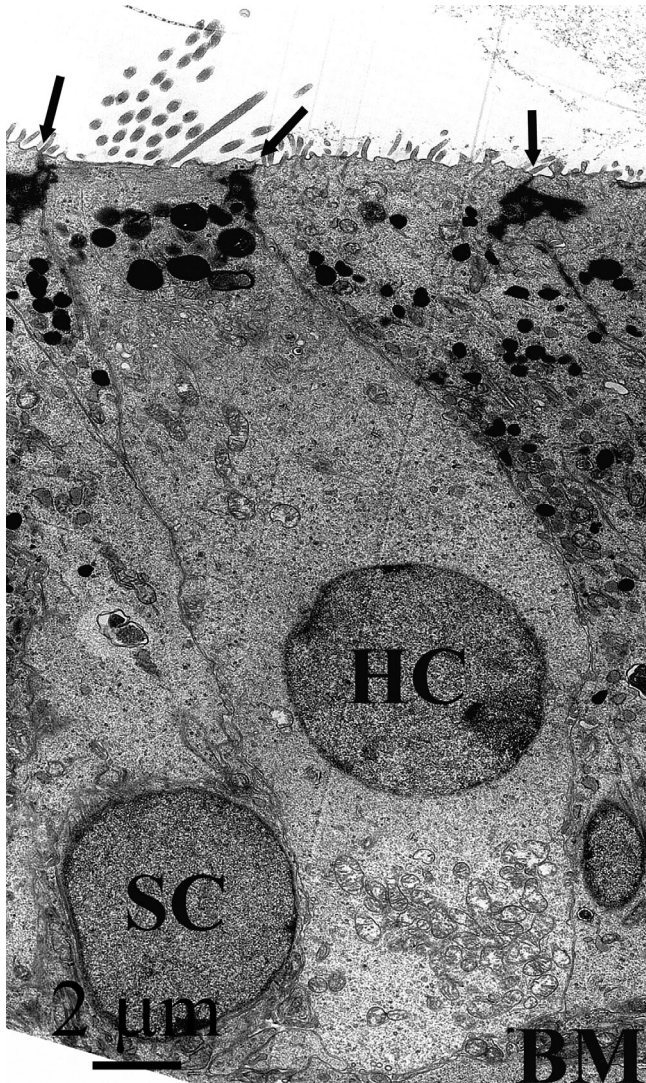
Fig. 6. A HC at 28 DIV from Group G with a stereocilia bundle and a distinct foot-process that reaches down to the basal membrane, and a basal accumulation of mitochondria. BM, basal membrane; black arrow points at a TJ between a HC and its neighboring SC.

Fig. 7. A HC at 28 DIV from Group G. BM, basal membrane; black arrow points at a TJ between a HC and its neighboring SC; asterix marks basal accumulation of mitochondria.

Observations of individual vestibular cells with some morphology signs characteristic for an HC and some morphology signs characteristic for an SC have been reported after trauma-induced HC-loss (Li and Forge, 1997; Werner et al., 2015). Cells that morphologically appear to be in an intermediate state between an SC and an HC have been reported to have stereocilia as an HC and basal extensions toward the basal membrane and sometimes seem to be covered apically by cytoplasmic extensions from neighboring SCs. In this study, a systematic characterization of these intermediate cells has been made. We found that both basal extensions toward the basal membrane and apical SC extensions covering the HC were more frequent in Group G than in Group C of macular specimens. Although apical SC extensions were more frequent in Group G than in Group C, there is a possibility that the apical part was not cut perpendicular to the HC giving a false impression of covering SC extensions. The correlation b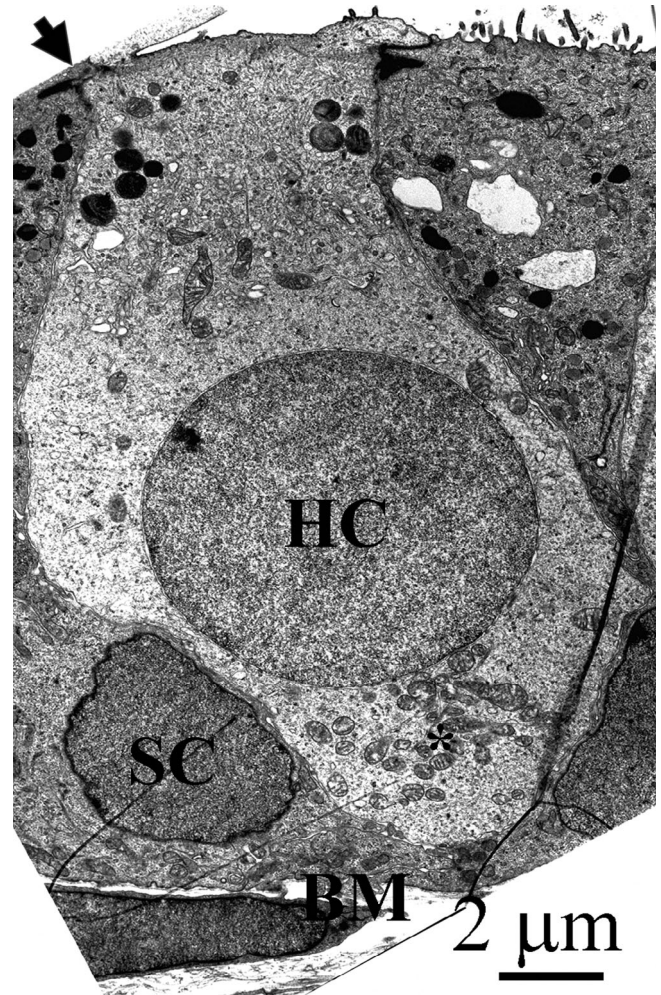etween the presence of apical SC extensions and the other characteristics in the same cell were weaker than for the other most frequent characteristics. Therefore, we conclude that apical SC extensions are a less reliable feature for identifying SCs that are transdifferentiating into HCs.

Interesting observations were the basal accumulation of mitochondria and that more than five visible connections with SCs also were more frequent in Group G specimens than in Group C. These observations have not been reported earlier.

Gap Junctions and Communicating Networks

Distinct GJ-like morphology could not be identified on either HCs or cells that seem to be in a transitional state between a SC and a HC. In a few transitional cells, short segments with GJ-like fusing of adjacent cell membranes were observed (Fig. 5). SCs have numerous areas along their cell membranes revealing a GJ-like morphology, and areas like this could easily be detected in our preparations also in utricles exposed to gentamicin (Fig. 12). These GJ-like areas detected between SCs differed greatly in length. Vesicles with double membranes
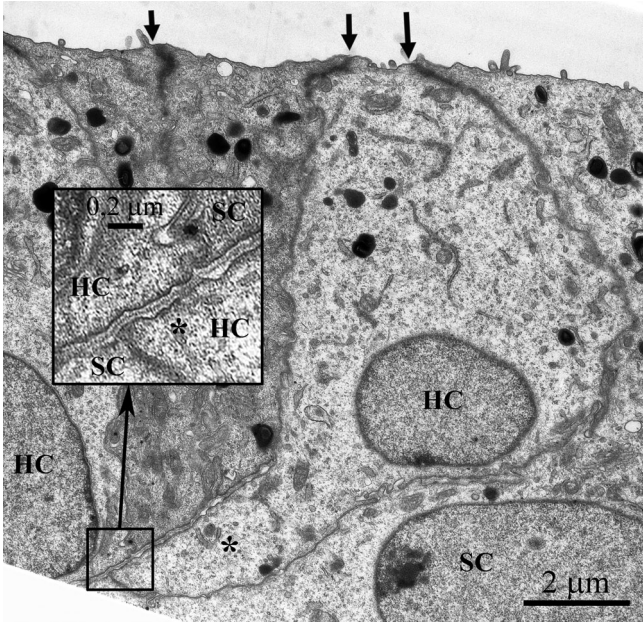
Fig. 8. A HC at 17 DIV from Group G with a basolateral extension connected to another HC. Black arrow points at a TJ between a HC and its neighboring SC; asterix marks basolateral extension of an HC.

possessing the morphological features of GJ plaques were found intracellularly in both SCs and HCs (Fig. 5). Intracellular GJ-like vesicles, i.e., annular GJs, have been described by others and are thought to indicate turnover of GJs in the cells where they are present (Jordan et al., 2001; Forge et al., 2003).

All the SCs in the inner ear of both birds and mammals seem to be functionally coupled through GJs to neighboring cells (Forge et al., 2003; Jagger and Forge, 2006; Nickel et al., 2006). The absence of GJs on HCs has led to the suggestion that HCs might function as independent units
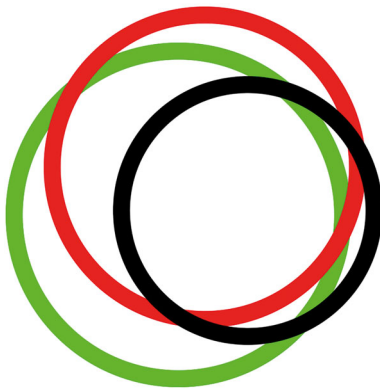

Fig. 9. Schematic illustration of the proportional occurrence of basal accumulation of mitochondria, foot process/basal extensions, or more than five SC connections with the HC, for HCs in Group G. Each circle represents the HCs showing the specific cell characteristic feature. The total number of examined HCs in Group G was 53. Green circle = basal accumulation of mitochondria (29 HCs); red circle = foot process/basal extensions (25 HCs); black circle = more than five SC connections (20 HCs). Eleven HCs showed all three features.
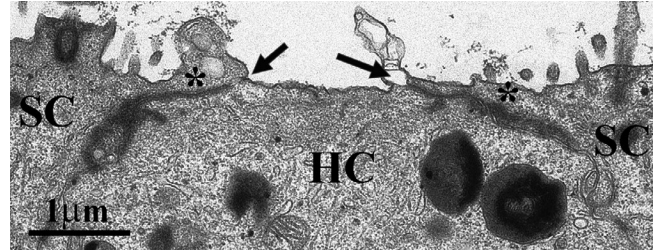

Fig. 10. Apical part of an HC at 28 DIV from Group G that is partly covered by apical extensions from neighboring SCs. Asterix marks extension of SC; black arrow points at a TJ between an HC and its neighboring SC.
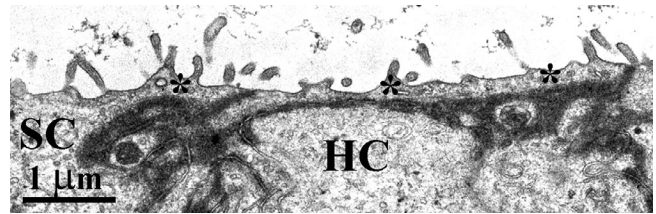

Fig. 11. Apical part of an HC at 21 DIV from Group G. The HC has no contact with the lumen and is covered by a thin layer of SC extensions. Asterix marks extension of SC.

(Forge et al., 2003). The only species where GJs have been associated with HCs are in the auditory and vestibular organs of the alligator lizard and gold fish (Nadol Jr. et al., 1976; Hama, 1980). Whether this represents the presence of functional differences between species is not known. Furthermore, there are recent reports of basolateral processes on Type II HCs in vestibular end organs from adult
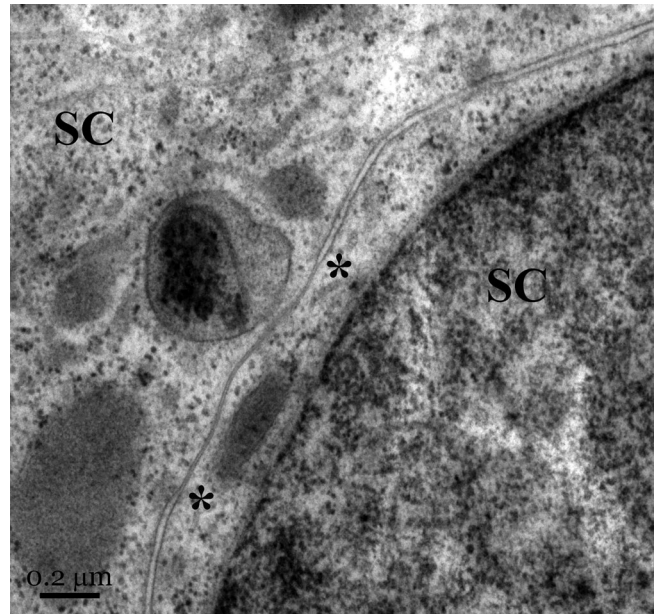

Fig. 12. GJ-like morphology of the cell membrane between two SCs in Group C after 21 DIV. Asterix marks the transition between ordinary cell membrane and GJ-like morphology.

mammals (Golub et al., 2012; Pujol et al., 2014). These basolateral processes contact one another, indicating a coupling between HCs. Using immunolabeling and imaging approaches Pujol and colleagues (23) were unable to identify basolateral processes in Type II HCs of adult rats. We have only identified one possible basolateral process in our study of perinatal rat utricular epithelia and this observation was done in a gentamicin-exposed explant (Fig. 8). The identification of basolateral processes is difficult in thin transverse sections and whether rats lack Type II HC processes has not yet been established.

Our results showing a lack of GJ-like morphology on transdifferentiating cells indicate that SCs destined to transdifferentiate into HCs leave the functionally coupling unit of the SC area at an early stage postaminoglycoside damage. The presence of intracellular GJ-like vesicles in HCs and the observations of short segments with GJ-like fusing of adjacent cell membranes in some transitional cells could be remnants of GJ turnover. Another possibility is that the group of SCs that retain the ability to directly transdifferentiate into HCs are less differentiated then the other SCs and do not participate in their communicating network.

Tight Junctional Seal and Adhesion Junctions

In gentamicin-exposed utricles, there are two processes that could possibly could cause disruption of the tight junctional seal toward the lumen and disruption of the adhesion between cells, namely, the death of HCs and the transdifferentiation of SCs.

We show that the tight junctional seals at the luminal border of HCs are morphologically intact at various time points *in vitro* both without and after gentamicin exposure.

The TJ seals seem to be morphological intact between all analyzed cells, with reference to both HC-to-SC and SC-to-SC connections. We did not find any morphological disruptions of the TJs between HCs, SCs, or cells with a transitional appearance at any of the analyzed time points. The earliest time point we analyzed in Group G was 2 DIV after gentamicin exposure. These findings are in concordance with earlier findings where no disruptions in the epithelial cell junctions was observed in vestibular epithelia in guinea pigs and gerbils (Li et al., 1995; Forge and Li, 2000) or in chick basilar papilla (Hirose et al., 2004) following gentamicin exposure. In contrast to these findings, morphological splitting of TJs and AJs has been described in vestibular epithelia between HCs and SCs 1 day after local neomycin treatment of 10-week-old mice (Kim et al., 2005). Three days after neomycin treatment of these 10-week-old mice Kim *et al.* (Bagger-Sjoback and Anniko, 1984) reported that abnormal morphology of TJs and AJs between HCs and SCs were frequent but 5 days after neomycin treatment TJs and AJs between HCs and SCs recovered to a normal state. Preservation of the permeability barrier after a sublethal injury to the HCs is a priority process (Kim et al., 2005). After HC injury, surrounding SCs form apical lateral extensions to seal the luminal border of the epithelia (Forge, 1985; Meiteles and Raphael, 1994; Taylor et al., 2012). A mechanism has been described in which adjacent SCs excise the dying HCs apical portion in order to form a new sealing TJ layer beneath the location of the original cuticular plate of the HC (Bucks et al., 2017; Gale et al., 2002; Li et al.,

1995; Forge, 1985). We did not see any excised apical parts of HCs in this study. However, we identified HCs that were covered apically with extensions from neighboring SCs. We observed some HCs covered with extensions from two neighboring SCs that were united with a TJ-like seal.

Both the HCs and cells with a transitional appearance showed characteristic junctional zonula of high electron density with TJs, AJs, and DSs in the apical lateral borders to the contiguous SCs. Further down along the lateral borders of these cells occasional DSs were found. The SCs also showed characteristic junctional zonula of high electron density with TJs, AJs, and DSs in the apical lateral borders to their neighboring SCs.

These findings with intact apical lining and continuous undisrupted cell borders and morphologically intact intercellular junctions indicate that preservation of the permeability barrier and that the integrity of cells is a priority process also during the process of direct transdifferentiation.

CONCLUSIONS

SCs transdifferentiating into HCs in gentamicin-exposed cultures of whole rat utricles are characterized by basal extensions, basal accumulation of mitochondria, and an increased amount of connections with SCs. No GJs were discernible at the ultrastructural level in cells identified as transitional cells, which can indicate that loss of GJs is an early event during the process of transdifferentiation from an SC into an HC. In these utricle cultures from postnatal rats, the tight junctional seal of the epithelia remains morphologically intact both before and after gentamicin exposure. Our ultrastructural observations of a cohort of transitional cells with specific features support the concept that a subpopulation of SCs present in the aminoglycoside-damaged utricular epithelia retains a limited stem cell capability to transdifferentiate into replacement HCs.

LITERATURE CITED

Bagger-Sjoback D, Anniko M. 1984. Development of intercellular junctions in the vestibular end-organ. A freeze-fracture study in the mouse. Ann Otol Rhinol Laryngol 93(1 Pt 1):89–95.

Berggren D, Liu W, Frenz D, Van De Water T. 2003. Spontaneous hair-cell renewal following gentamicin exposure in postnatal rat utricular explants. Hear Res 180(1–2):114–125.

Bramhall NF, Shi F, Arnold K, Hochedlinger K, Edge AS. 2014. Lgr5-positive supporting cells generate new hair cells in the postnatal cochlea. Stem cell reports 2(3):311–322.

Bucks SA, Cox BC, Vlosich BA, Manning JP, Nguyen TB, Stone JS. 2017. Supporting cells remove and replace sensory receptor hair cells in a balance organ of adult mice. Elife 6. pii: e18128. https://doi.org/10.7554/eLife.18128.

Burns JC, Stone JS. 2017. Development and regeneration of vestibular hair cells in mammals. Semin Cell Dev Biol 65:96–105.

Cox BC, Chai R, Lenoir A, Liu Z, Zhang L, Nguyen DH, Chalasani K, Steigelman KA, Fang J, Rubel EW, et al. 2014. Spontaneous hair cell regeneration in the neonatal mouse cochlea in vivo. Development 141(4):816–829.

Forge A. 1985. Outer hair cell loss and supporting cell expansion following chronic gentamicin treatment. Hear Res 19(2):171–182.

Forge A, Li L. 2000. Apoptotic death of hair cells in mammalian vestibular sensory epithelia. Hear Res 139(1–2):97–115.

Forge A, Li L, Corwin JT, Nevill G. 1993. Ultrastructural evidence for hair cell regeneration in the mammalian inner ear. Science 259 (5101):1616–1619.

Forge A, Li L, Nevill G. 1998. Hair cell recovery in the vestibular sensory epithelia of mature guinea pigs. J Comp Neurol 397(1):69–88.

Forge A, Becker D, Casalotti S, Edwards J, Marziano N, Nevill G. 2003. Gap junctions in the inner ear: comparison of distribution patterns in different vertebrates and assessement of connexin composition in mammals. J Comp Neurol 467(2):207–231.

Gale JE, Meyers JR, Periasamy A, Corwin JT. 2002. Survival of bundleless hair cells and subsequent bundle replacement in the bullfrog's saccule. J Neurobiol 50(2):81–92.

Golub JS, Tong L, Ngyuen TB, Hume CR, Palmiter RD, Rubel EW, Stone JS. 2012. Hair cell replacement in adult mouse utricles after targeted ablation of hair cells with diphtheria toxin. J Neurosci 32 (43):15093–15105.

Hama K. 1980. Fine structure of the afferent synapse and gap junctions on the sensory hair cell in the saccular macula of goldfish: a freeze-fracture study. J Neurocytol 9(6):845–860.

Hirose K, Westrum LE, Cunningham DE, Rubel EW. 2004. Electron microscopy of degenerative changes in the chick basilar papilla after gentamicin exposure. J Comp Neurol 470(2):164–180.

Jagger DJ, Forge A. 2006. Compartmentalized and signal-selective gap junctional coupling in the hearing cochlea. J Neurosci 26(4): 1260–1268.

Jagger DJ, Nickel R, Forge A. 2014. Gap junctional coupling is essential for epithelial repair in the avian cochlea. J Neurosci 34(48): 15851–15860.

Jordan K, Chodock R, Hand AR, Laird DW. 2001. The origin of annular junctions: a mechanism of gap junction internalization. J Cell Sci 114(Pt 4:763–773.

Kawamoto K, Izumikawa M, Beyer LA, Atkin GM, Raphael Y. 2009. Spontaneous hair cell regeneration in the mouse utricle following gentamicin ototoxicity. Hear Res 247(1):17–26.

Kim TS, Nakagawa T, Kitajiri S, Endo T, Takebayashi S, Iguchi F, Kita T, Tamura T, Ito J. 2005. Disruption and restoration of cell-cell junctions in mouse vestibular epithelia following aminoglycoside treatment. Hear Res 205(1–2):201–209.

King DG, Kammlade N, Murphy J. 1982. A simple device to help re-embed thick plastic sections. Stain Technol 57(5):307–310.

Li L, Forge A. 1997. Morphological evidence for supporting cell to hair cell conversion in the mammalian utricular macula. Int J Dev Neurosci 15(4–5):433–446.

Li L, Nevill G, Forge A. 1995. Two modes of hair cell loss from the vestibular sensory epithelia of the guinea pig inner ear. J Comp Neurol 355(3):405–417.

Lin V, Golub JS, Nguyen TB, Hume CR, Oesterle EC, Stone JS. 2011. Inhibition of Notch activity promotes nonmitotic regeneration of hair cells in the adult mouse utricles. J Neurosci 31(43):15329–15339.

Lin J, Zhang X, Wu F, Lin W. 2015. Hair cell damage recruited Lgr5-expressing cells are hair cell progenitors in neonatal mouse utricle. Front Cell Neurosci 9:113.

Meiteles LZ, Raphael Y. 1994. Scar formation in the vestibular sensory epithelium after aminoglycoside toxicity. Hear Res 79(1–2):26–38.

Nadol JB Jr, Mulroy MJ, Goodenough DA, Weiss TF. 1976. Tight and gap junctions in a vertebrate inner ear. Am J Anat 147(3): 281–301.

Nickel R, Becker D, Forge A. 2006. Molecular and functional characterization of gap junctions in the avian inner ear. J Neurosci 26 (23):6190–6199.

Pujol R, Pickett SB, Nguyen TB, Stone JS. 2014. Large basolateral processes on type II hair cells are novel processing units in mammalian vestibular organs. J Comp Neurol 522(14):3141–3159.

Tanyeri H, Lopez I, Honrubia V. 1995. Histological evidence for hair cell regeneration after ototoxic cell destruction with local application of gentamicin in the chinchilla crista ampullaris. Hear Res 89 (1–2):194–202.

Taylor RR, Jagger DJ, Forge A. 2012. Defining the cellular environment in the organ of Corti following extensive hair cell loss: a basis for future sensory cell replacement in the Cochlea. PloS One 7(1): e30577.

Werner M, Van De Water TR, Hammarsten P, Arnoldsson G, Berggren D. 2015. Morphological and morphometric characterization of direct transdifferentiation of support cells into hair cells in ototoxin-exposed neonatal utricular explants. Hear Res 321:1–11.